NASA/TM—2006-214363

Comparison of Atomic Oxygen Erosion Yields of Materials at Various Energy and Impact Angles

Bruce A. Banks
Glenn Research Center, Cleveland, Ohio

Deborah L. Waters
QSS Group, Inc., Cleveland, Ohio

Stephen D. Thorson
University of Wisconsin at Madison
Madison, Wisconsin

Kim K. deGroh, Aaron Snyder, and Sharon Miller
Glenn Research Center, Cleveland, Ohio

August 2006

NASA STI Program . . . in Profile

Since its founding, NASA has been dedicated to the advancement of aeronautics and space science. The NASA Scientific and Technical Information (STI) program plays a key part in helping NASA maintain this important role.

The NASA STI Program operates under the auspices of the Agency Chief Information Officer. It collects, organizes, provides for archiving, and disseminates NASA's STI. The NASA STI program provides access to the NASA Aeronautics and Space Database and its public interface, the NASA Technical Reports Server, thus providing one of the largest collections of aeronautical and space science STI in the world. Results are published in both non-NASA channels and by NASA in the NASA STI Report Series, which includes the following report types:

- TECHNICAL PUBLICATION. Reports of completed research or a major significant phase of research that present the results of NASA programs and include extensive data or theoretical analysis. Includes compilations of significant scientific and technical data and information deemed to be of continuing reference value. NASA counterpart of peer-reviewed formal professional papers but has less stringent limitations on manuscript length and extent of graphic presentations.

- TECHNICAL MEMORANDUM. Scientific and technical findings that are preliminary or of specialized interest, e.g., quick release reports, working papers, and bibliographies that contain minimal annotation. Does not contain extensive analysis.

- CONTRACTOR REPORT. Scientific and technical findings by NASA-sponsored contractors and grantees.

- CONFERENCE PUBLICATION. Collected papers from scientific and technical conferences, symposia, seminars, or other meetings sponsored or cosponsored by NASA.

- SPECIAL PUBLICATION. Scientific, technical, or historical information from NASA programs, projects, and missions, often concerned with subjects having substantial public interest.

- TECHNICAL TRANSLATION. English-language translations of foreign scientific and technical material pertinent to NASA's mission.

Specialized services also include creating custom thesauri, building customized databases, organizing and publishing research results.

For more information about the NASA STI program, see the following:

- Access the NASA STI program home page at *http://www.sti.nasa.gov*

- E-mail your question via the Internet to *help@sti.nasa.gov*

- Fax your question to the NASA STI Help Desk at 301–621–0134

- Telephone the NASA STI Help Desk at 301–621–0390

- Write to:
  NASA STI Help Desk
  NASA Center for AeroSpace Information
  7121 Standard Drive
  Hanover, MD 21076–1320

NASA/TM—2006-214363

Comparison of Atomic Oxygen Erosion Yields of Materials at Various Energy and Impact Angles

Bruce A. Banks
Glenn Research Center, Cleveland, Ohio

Deborah L. Waters
QSS Group, Inc., Cleveland, Ohio

Stephen D. Thorson
University of Wisconsin at Madison
Madison, Wisconsin

Kim K. deGroh, Aaron Snyder, and Sharon Miller
Glenn Research Center, Cleveland, Ohio

Prepared for the
10th International Symposium on Materials in a Space Environment (ISMSE) cosponsored by the ONERA, CNES, and ESA
and the 8th International Conference on the Protection of Materials and Structures in a Space Environment (ICPMSE) organized by ITL, Inc., and the CSA
Collioure, France, June 19–23, 2006

National Aeronautics and
Space Administration

Glenn Research Center
Cleveland, Ohio 44135

August 2006

Level of Review: This material has been technically reviewed by technical management.

Available from

NASA Center for Aerospace Information
7121 Standard Drive
Hanover, MD 21076–1320

National Technical Information Service
5285 Port Royal Road
Springfield, VA 22161

Available electronically at http://gltrs.grc.nasa.gov

Comparison of Atomic Oxygen Erosion Yields of Materials at Various Energy and Impact Angles

Bruce A. Banks
National Aeronautics and Space Administration
Glenn Research Center
Cleveland, Ohio 44135

Deborah L. Waters
QSS Group, Inc.
Cleveland, Ohio 44135

Stephen D. Thorson
University of Wisconsin at Madison
Madison, Wisconsin 53711

Kim K. deGroh, Aaron Snyder, and Sharon Miller
National Aeronautics and Space Administration
Glenn Research Center
Cleveland, Ohio 44135

Abstract

The atomic oxygen erosion yields of various materials, measured in volume of material oxidized per incident atomic oxygen atom, are compared to the commonly accepted standard of Kapton H (DuPont) polyimide. The ratios of the erosion yield of Kapton H to the erosion yield of various materials are not consistent at different atomic oxygen energies. Although it is most convenient to use isotropic thermal energy RF plasma ashers to assess atomic oxygen durability, the results can be misleading because the relative erosion rates at thermal energies are not necessarily the same as low Earth orbital (LEO) energies of ~4.5 eV. An experimental investigation of the relative atomic oxygen erosion yields of a wide variety of polymers and carbon was conducted using isotropic thermal energy (~0.1 eV) and hyperthermal energy (~70 eV) atomic oxygen using an RF plasma asher and an end Hall ion source. For hyperthermal energies, the atomic oxygen erosion yields relative to normal incident Kapton H were compared for sweeping atomic oxygen arrival with that of normal incidence arrival. The results of isotropic thermal energy, normal incident, and sweeping incident atomic oxygen are also compared with measured or projected LEO values.

1. Introduction

The atomic oxygen erosion yields of hydrocarbon and halocarbon polymers relative to Kapton H polyimide have been found to differ between measurements in low Earth orbit (LEO) and those in ground based simulation facilities (refs. 1 to 3). For example the erosion yield of fluorinated ethylene propylene Teflon, polyethylene, and pyrolytic graphite has been found to be 11.2, 110, and 40 percent of that of Kapton H polyimide in LEO (ref. 3) respectively but is 55.8, 288, and 72 percent that of Kapton H polyimide respectively in an RF plasma asher (ref. 1). It is fully expected that other polymers will also differ in relative erosion yield between LEO and RF plasma asher environments. Thus, it is desirable to be able to quantify the relative rates (using Kapton H polyimide as the reference material) in both environments to allow one to meaningfully project LEO durability of components based on low cost laboratory RF plasmas.

To help provide understanding of atomic oxygen erosion yield energy dependencies, a similar comparison of relative erosion yields at hyperthermal energies can similarly be accomplished using an end Hall atomic oxygen ion source (also with Kapton H polyimide as the reference material) which operates at ~70 eV (ref. 4).

Atomic oxygen attack of most spacecraft surfaces occurs in a sweeping manner in which the angle of attack changes as the spacecraft orbits the Earth. This sweeping attack should cause a less prominent texture than for normal incidence. In normal incidence, the typical cones that form should allow multiple opportunities for scattered atomic oxygen to react. In contrast, for sweeping incidence, the reduced height cones or rills should reduce the reaction probability of incoming atomic oxygen. Thus, one would expect a reduction in erosion yield for sweeping incidence unless there is an increase in reaction probability off normal angles of attack. In addition, a portion of each orbit has atomic oxygen arriving at near grazing angles of incidence. One of the objectives of this investigation is to compare the atomic oxygen erosion yield at hyperthermal energies for normal incidence with that of sweeping incidence.

2. Apparatus and Procedure

The atomic oxygen erosion measurement techniques followed the protocols designated in the ASTM procedure E 2089-00 for Standard Practices for Ground Laboratory Atomic Oxygen Interaction Evaluation of Materials for Space Applications. The atomic oxygen erosion yield was determined knowing the density of the materials, the Kapton H polyimide effective fluence and by measuring weight loss in samples immediately after removal from vacuum desiccators after at least 48 hr of vacuum exposure at ~100 μm (13.3 Pa) to assure that variability in mass due to absorbed water would not compromise the weight loss measurements. The atomic oxygen Kapton H effective fluence was similarly measured using the density of 1.42 gm/cm^3 and a LEO erosion yield, E_K, of 3.0×10^{-24} cm^3/atom for Kapton H fluence witness samples (ref. 4). For test samples and Kapton H fluence witness samples of equal areas, the erosion yield, E_S, for the test samples (exposed to the same fluence levels) is given by

$$E_S = \frac{\Delta M_S \rho_K}{\Delta M_K \rho_S} E_K$$

where ΔM_S = mass loss of the test sample

ΔM_K = mass loss of the Kapton H fluence witness sample

ρ_S = density of the test sample

ρ_K = density of the Kapton H fluence witness sample

Thermal energy atomic oxygen exposure of samples was accomplished using a Plasma Prep II, 13.56 MHz RF plasma asher operated on air at 100 W and ~100 μm (13.3 Pa) pressure.

Hyperthermal energy atomic oxygen exposure at normal and sweeping incidence was accomplished using a Veeco end Hall ion source operated on 100 percent oxygen in a background pressure of 10^{-4} torr (1.33×10^{-2} Pa) during operation with an anode voltage of 90 eV and an anode current of 3.5 amperes. This produced a beam of almost exclusively O_2^+ with negligible O^+ or O^{++} ions as measured by an E x B probe by James R. Kahn and Raymond S. Robinson, of Front Range Research, Fort Collins, CO Sept. 28, 1989. The energy distribution contained two distinct energy peaks (one at ~40 eV and one at ~85 eV) which resulted in an average energy of ~70 eV (ref. 5). A water-cooled thermal radiation shield was used over the lower half of the end Hall source to shield samples located downstream and prevent sample heating from the heat radiated by the end Hall source cathode Fig. 1.

Sweeping atomic oxygen was accomplished by means of a rotating paddle shaped sample holder which was located 56.5 cm downstream of the end Hall source and driven by a chain powered by a rotating shaft which used a ferro-fluid seal through the vacuum system wall to an external stepper motor Fig. 1.

The rotating sample holder had 11 samples mounted on each side of it. It was rotated at ~1 rpm. Samples were 2.54 cm in diameter and of various thicknesses ranging from 0.0254 to 1.0 mm thick and mounted

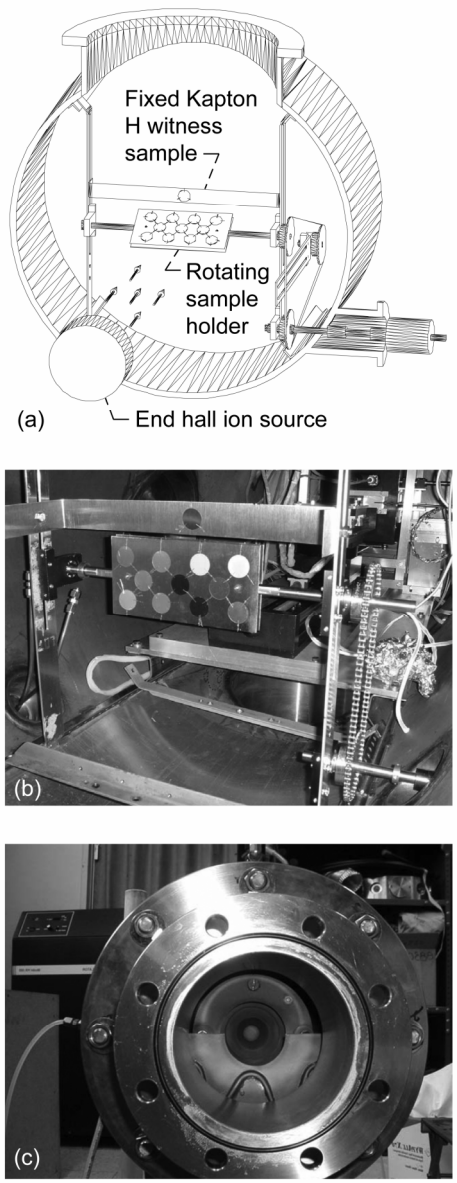

Fig. 1. Sample holder and end Hall atomic oxygen source configuration for normal and sweeping incident atomic oxygen exposure. (a) Drawing. (b) Photograph of sample sweeping mechanism with samples mounted on the rotating holder and fixed Kapton H witness holder. (c) Photograph of end Hall atomic oxygen source.

using three or four small diameter (0.51 mm) wires to hold the samples in place yet minimize the occlusion of the atomic oxygen arrival. The area protected by the wires is estimated to be 1.3 percent of the area for samples exposed to normal incidence with three wires used to hold the samples and 1.7 percent for four-wire sample mounts. These protection considerations were taken into account for sweeping incidence where the protected areas represent 5.4 percent of the area of the three-wire holder samples and 7.8 percent of the four-wire holder samples. However, to compare erosion yields for normal incidence compared to sweeping fluence one must also take into account the cosine of the arrival angle relative to normal which causes an additional reduction in fluence by a factor of π. This causes the fluence for the three-wire mounted sweeping samples to be 30.1 percent of the normal unobstructed incident fluence and 29.3 percent for the four-wire mounted samples. To allow a comparison of the fluence measurement at normal and at sweeping incidence, a normal incident Kapton H polyimide fluence witness sample was placed above the rotating sample holder and without rotating it). This enabled an effective fluence to a set of Kapton H witness samples was placed at all the sample locations on of the rotating sample holder (but be projected for every sample location based on the fixed witness sample for both normal incident and sweeping arrival. The samples were arranged in three rows on both sides of the rotating sample holder.

The choice of samples to be tested was based on polymers of interest for spacecraft use but included pyrolytic graphite with atomic oxygen arrival being isotropic, perpendicular or sweeping with respect to the graphene plane. Table I lists the materials, abbreviations, trade names, density, erosion yields, and atomic fraction of the elements that each material is composed of for the materials tested.

The erosion yields listed in Table I, are those determined from in-space exposures on the Long Duration Exposure Facility (for polyimide Kapton H) or recently retrieved results from a four year exposure on the International Space Station (for all the remaining polymers) (refs. 6 to 7). The densities listed are literature values for Kapton CB (black polyimide), Lupolen (polyethylene) Nomex (polyphenylene isophthalate), and pyrolytic graphite but density

TABLE I.—MATERIALS TESTED AND THEIR ABBREVIATIONS, TRADE NAMES, DENSITIES, AND LEO EROSION YIELDS

					Atomic percent						
Material	Abbrev.	Trade name	Density, gm/cm^3	LEO Erosion yield, $x\ 10^{-24}$ $cm^3/atom$	H	C	N	O	F	S	Cl
Polyimide H (PMDA)	PI-H	Kapton H	1.427	3.0	26	56	5	13	0	0	0
Polyimide-HN (PMDA)	PI-HN	Kapton HN	1.435	2.81	26	56	5	13	0	0	0
Black polyimide	Black PI	Kapton CB	1.42	?	?	?	?	?	0	0	0
Pyrolytic graphite	PG	----------	2.22	0.415	0	100	0	0	0	0	0
Fluorinated ethylene propylene	FEP	Teflon FEP	2.144	0.200	0	33	0	0	67	0	0
Ethylene chlorotrifluoro-ethylene	ECTFE	Halar	1.676	1.79	33	33	0	0	25	0	8
Polycarbonate	PC	Lexan	1.123	4.29	42	48	0	9	0	0	0
Chlorotrifluoroethylene	CTFE	Aclar Kel-f	2.133	0.831	0	33	0	0	50	0	17
Polyethylene	PE	Lupolen	0.918	3.97	67	33	0	0	0	0	0
Polyethylene terephthalate	PET	Mylar A200	1.393	3.01	38	48	0	14	0	0	0
Polyoxymethylene	POM	Delrin	1.398	9.14	50	25	0	25	0	0	0
Polyphenylene isophthalate	PPPA	Nomex	0.72	1.41	36	50	7	7	0	0	0
Polypropylene	PP	Profax	0.907	2.68	67	33	0	0	0	0	0
Polysulphone	PSU	Udel	1.220	2.94	41	50	0	7	0	2	0
Polytetrafluoroethylene	PTFE	Teflon PTFE	2.150	0.142	0	33	0	0	67	0	0
Polyvinyl fluoride	PVF	Tedlar	1.379	3.19	50	33	0	0	17	0	0
Polyvinylidene fluoride	PVDF	Kynar	1.762	1.29	33	33	0	0	33	0	0
Polytetrafluoroethylene ethylene copolymer	ETFE	Tefzel ZM	1.740	.961	33	33	0	0	33	0	0

gradient column measurements of the actual polymers tested of for the remaining materials (ref. 7).

Monte Carlo computational modeling of the normal incident and sweeping incident AO erosion was performed to explore if the erosion yield arrival dependence that was experimentally observed was consistent with results of computational modeling where a random texture also develops. This was performed using the computational methods and parameters given in (ref. 3).

3. Results and Discussion

For the thermal energy RF plasma asher tests, samples were exposed to Kapton H effective fluences ranging from 5×10^{19} to 1.5×10^{21} atoms/cm^2 depending on the thickness of the sample to assure that the sample was significantly eroded but not to an extent that would cause it to erode completely through its thickness. The flux map for fixed orientation samples placed in the RF plasma ashers is shown in Fig. 2.

The fluxes shown in Fig. 2 are all relative to the flux measured by the Kapton H fluence witness sample. The flux map for the samples placed on a larger sample holder in the hyperthermal energy end Hall facility is shown in Fig 3.

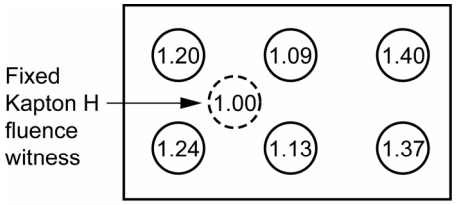

Fig. 2. Flux map (relative to Kapton H) for samples tested in the thermal energy RF plasma asher.

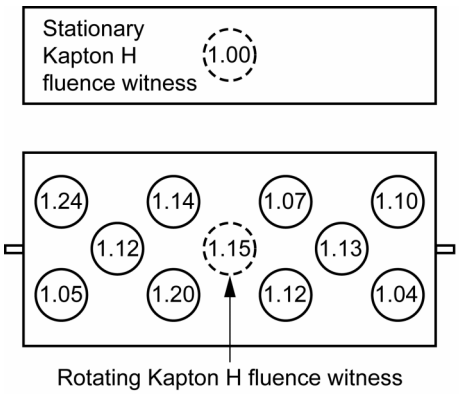

Fig. 3. Flux map (relative to stationary Kapton H of samples placed in the hyperthermal energy end Hall facility.

The flux was measured without sample holder rotation. The samples were exposed for 12 hr to accumulate a total fluence of 1.64×10^{20}atoms/cm^2 on the Kapton H fluence witness sample. The resulting erosion yields of the various materials relative to Kapton H polyimide are given in Table II for thermal energy RF plasma exposure (~0.1 eV) and fixed (non-rotating) normal incident hyperthermal energy (~70 eV) atomic oxygen.

TABLE II.—EROSION YIELDS RELATIVE TO KAPTON H

Material	Erosion yield relative to Kapton H for each energy range		
	Thermal energy RF plasma, ~0.1 eV	In LEO, ~4.5 eV	Hyperthermal energy, from end Hall source, ~70 eV
PI-H	1	1	1
PI-HN	0.90	0.937	1.03
Black PI	0.88	unknown	0.90
PG	0.61	0.138	0.58
FEP	0.81	0.067	1.89
ECTFE	0.83	0.597	1.59
PC	2.52	1.43	1.07
CTFE	1.19	0.277	2.86
PE	1.65	1.25	1.06
PET	1.09	1.00	1.30
POM	12.20	3.05	10.87
PPPA	2.18	0.470	1.47
PP	2.99	1.23	1.40
PSU	1.49	0.980	0.98
PTFE	0.39	0.047	1.86
PVF	1.79	1.06	1.10
PVDF	0.42	0.430	1.42
ETFE	0.74	0.320	1.08

It is interesting to note from the table that there is not a consistent energy dependent prediction of erosion yields based on the data from ~70 eV O_2^+ ions based, ~0.1 eV thermal energy plasmas and space ~4.5 eV hyperthermal O atoms. Thus, one cannot, in general, simply draw a consistent curve of erosion yield versus energy for all materials to predict in-space atomic oxygen erosion based on ground laboratory data from oxygen at energies above and below the LEO energy of interest. At hyperthermal energies of ~70 eV, there does not seem to be a clear or simple chemical composition dependence upon the erosion yield relative to Kapton H at ~4.5 eV LEO energies. Thus, prediction of in-space durability, based on arbitrary-energy ground laboratory testing, will require in-space validation until an erosion yield dependence can be established which takes into account the atomic oxygen energy and material chemistry.

The average erosion yield of the various polymers relative to Kapton H for each energy range is shown in Table III. As can be seen in Table III, the erosion yields

relative to Kapton H is lowest for halogenated polymers at any energy range. Both the asher and end Hall exposures involve ions and plasmas which may also play a roll when comparing to the LEO environment. The standard deviations listed are high relative to the average values which are simply indicative of the wide variation in erosion yields for the various materials. The extremely high erosion yield of polyoxymethylene is the prime contributor to the high standard deviation in erosion yields.

TABLE III.—EROSION YIELD OF VARIOUS CHEMISTRY MATERIALS RELATIVE TO KAPTON H FOR VARIOUS ENERGY AO

Material	Erosion yield relative to Kapton H for each energy range		
	RF plasma at thermal energy, ~0.1 eV	In LEO, ~4.5 eV	End Hall source hyperthermal energy, ~70 eV
Average of non-halogenated polymers and carbon	2.5 ±3.3	1.1 ±0.8	2.0 ±2.7
Average of all halogenated polymers	0.9 ±0.5	0.8 ±0.4	1.9 ±0.6
Average of all polymers and carbon	1.9 ±2.7	0.1 ±0.7	1.9 ±2.3

The erosion yields for sweeping atomic oxygen arrival relative to fixed-arrival normal incident hyperthermal atomic oxygen on Kapton H are given in Table IV. As can be seen from Table IV, except for polyoxymethylene and polyvinyl fluoride all materials have a greater erosion yield when in a sweeping atomic oxygen exposure. For the entire list of materials, the average ratio of sweeping to normal-incident fixed-arrival atomic oxygen erosion yields is 1.12. The variation in sample-to-source separation can only account for less than 0.03 percent of the increase of 12 percent in sweeping erosion yield over normal-incident fixed-arrival atomic oxygen erosion yield. The standard deviation in fractional uncertainty in the ratio of sweeping erosion yield to normal-incident erosion yield for a typical polymer such as Kapton H was found to be 14 percent and the standard deviation for the average of all the materials was 20 percent. Thus, the 12 percent increase in sweeping erosion yield over normal-incident erosion yield is within the experimental error. However, one is still tempted to wonder of some aspect of the sweeping atomic oxygen attack causes greater erosion than normal incident attack. Erosion yield dependence upon arrival angle and/or changing directions of the development of surface texturing may play a roll in the increase in oxidation.

Monte Carlo computational modeling of the Kapton H normal incident and sweeping incident erosion was performed to the same fluence levels as for the experimental testing to explore if the erosion yield sweeping-dependence was consistent with the texture that is developed by the computational modeling using the computational methods and parameters of (ref. 3). The computational results were computed for the identical fluences experimentally tested. These results, for Kapton H, showed that the ratio of sweeping to normal incident erosion yield was 0.82±0.075, which was lower than normal incidence in contrast to the experimentally observed results. However, this was more consistent with what would be expected due to surface texture induced trapping of the incident atomic oxygen. Such effects would tend to increase the erosion yield of highly textured normal incident samples in comparison with lower textured sweeping samples. It is also not clear whether the surprising reduction in relative erosion rates for polyoxymethylene and polyvinyl fluoride under sweeping conditions, shown in Table IV are erroneous data points or are real for some unknown reason.

TABLE IV.—COMPARISON OF RELATIVE EROSION YIELDS OF NORMAL INCIDENT AND SWEEPING INCIDENT ATOMIX OXYGEN AT ~70 EV FROM AN END HALL ION SOURCE

Material	Erosion yield relative to Kapton H		Ratio of sweeping to normal incident erosion yields for the same material
	With normal incidence hyperthermal energy AO	With sweeping incidence hyperthermal energy AO	
PI-H	1	1.100	1.100
PI-HN	1.03	1.130	1.097
Black PI	0.90	1.003	1.114
PG	0.58	0.699	1.204
FEP	1.89	Sample fell from mount	Sample fell from mount
ECTFE	1.59	1.813	1.140
PC	1.07	1.230	1.150
CTFE	2.86	3.666	1.282
PE	1.06	1.398	1.318
PET	1.30	1.593	1.226
POM	10.87	8.372	0.770
PPPA	1.47	1.664	1.132
PP	1.40	1.517	1.084
PSU	0.98	1.098	1.120
PTFE	1.86	2.467	1.326
PVF	1.10	0.511	0.464
PVDF	1.42	1.528	1.076
ETFE	1.08	1.595	1.477
Average of all materials	1.91 ±2.4	1.91 ±1.81	1.12 ±0.23

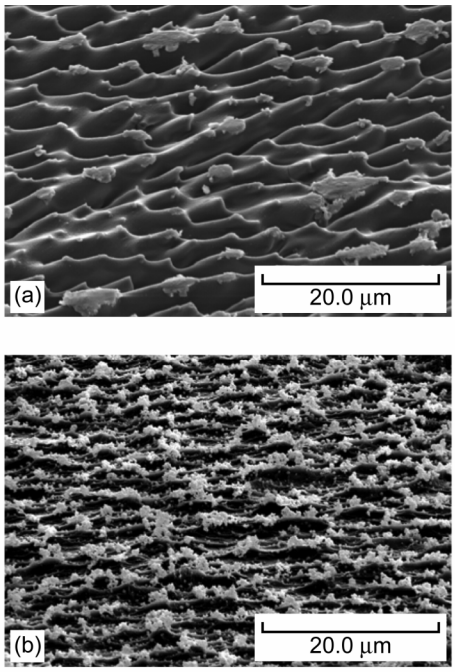

Fig. 4. Scanning electron microscope images after sweeping atomic oxygen attack showing a mix of columnar and rill structures. (a) Fluorinated ethylene propylene exposed space on the Hubble Space Telescope solar array drive arm. (b) Polyoxymethylene exposed to sweeping atomic oxygen from an end Hall ion source.

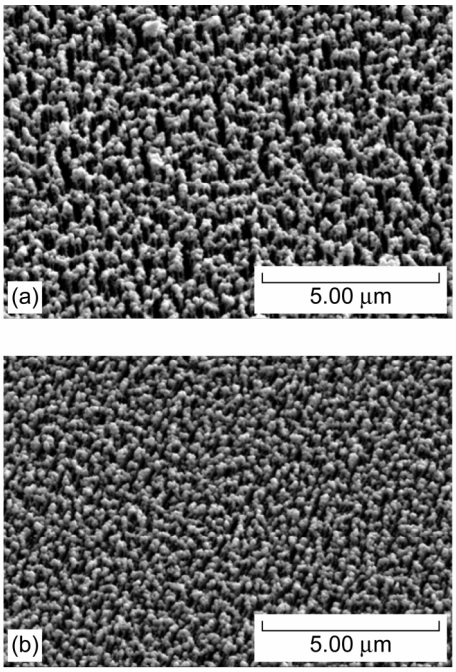

Fig. 5. Scanning electron microscope images of polymers exposed to sweeping incident arrival hyperthermal atomic oxygen exposure from an end Hall atomic oxygen source showing only columnar structures. (a) Polyethylene terephthalate (Mylar). (b) Polyimide (Kapton H).

It is interesting to note that the surface texture that typically results from normal incident LEO atomic oxygen exposure is different for hyperthermal sweeping atomic oxygen exposure than for fixed arrival a normal incidence for some but not all materials. As can be seen from Fig. 4, for fluorinated ethylene propylene exposed to sweeping atomic oxygen in space on the Hubble Space Telescope solar array drive arm and polyoxymethylene exposed to sweeping atomic oxygen from an end Hall ion source produce a mix of columnar and rill structures. However, for polyethylene terephthalate (Mylar) and polyimide (Kapton H) under sweeping incidence by an end Hall ion source, there appears to be only columnar structures Fig. 5.

4. Summary

A wide variety of polymers and carbon were exposed in thermal energy atomic oxygen in RF plasma ashers and to hyperthermal atomic oxygen in an end Hall atomic oxygen facility. The hyperthermal atomic oxygen impinged on samples at normal incidence and under sweeping arrival conditions. The erosion yields relative to Kapton H in each laboratory environment are reported as well as relative to referenced erosion yields measured in LEO.

The energy of atomic oxygen arrival may have a significant influence on the erosion yield of materials relative to Kapton H. At thermal energies in RF plasma ashers, materials with high chlorine or fluorine atomic contents have anomalously high erosion yields relative to in the LEO environment. However, at hyperthermal energies of ~70 eV, there does not seem to be a clear or simple chemical composition dependence upon the erosion yields relative to Kapton H at LEO energies. Presence of ions or immersion in a plasma may also play a role in differences between LEO and ground laboratory exposures. Thus, prediction of in-space tomic oxygen durability based on ground laboratory testing requires knowledge of the actual in-space erosion yield of a material until a clear erosion yield dependence can be validated based on atomic oxygen energy and material chemistry.

Sweeping hyperthermal atomic oxygen produces an average of 12 percent increase in erosion yield over normal-incident fixed-arrival atomic oxygen erosion yield for most of the materials tested. However, the 12 percent increase in erosion yield was within the 14 percent standard deviation of the experimental error.

Only two materials, polyoxymethylene and polyvinyl fluoride, have lower erosion yields when in a sweeping atomic oxygen exposure than in a normal-incident fixed-arrival atomic oxygen exposure.

For some, but not all, polymers sweeping atomic oxygen attack cause both rill formations superimposed on the pillar formation that is normally present for normal fixed incident atomic oxygen.

References

1. Rutledge, S.K., Banks, B.A. and Cales, M., "A Comparison of Atomic Oxygen Erosion Yields of Carbon and Selected Polymers Exposed in Ground Based Facilities and in Low Earth Orbit," NASA TM 1006622, paper presented at the AIAA Aerospace Ground Testing Conference, Colorado Springs, CO, June 20–23, 1994.
2. Rutledge, S.K., Banks, B.A., and Kitral, M., "A Comparison of Space and Ground Based Facility Environmental Effects for FEP Teflon," paper presented at the Fourth International Space Conference, ICPMSE–4, Toronto, Canada, April 23–24, 1998.
3. Banks, Bruce A., de Groh, Kim K., and Miller, Sharon K., "Low Earth Orbital Atomic Oxygen Interactions with Spacecraft Materials," NASA/TM—2004-213400 and paper presented at the Fall 2004 Meeting of the Materials Research Society, Boston Massachusetts, November 29-December 3, 2004.
4. Dever, Joyce, Banks, Bruce, de Groh, Kim, and Miller, Sharon, "Degradation of Spacecraft Materials", in Handbook of Environmental Degradation of Materials, Chapter 23, pp. 465–501, published by William Andrew Publishing, Norwich, NY, 2005.
5. James R. Kahn and Raymond S. Robinson, NASA contract report, Front Range Research, Fort Collins, CO, September 28, 1989.
6. Banks, B.A., Chapter 4, entitled, "The Use of Fluoropolymers in Space Applications," in Modern Fluoropolymers: High Performance Polymers for Diverse Applications, edited by J. Scheirs, John Wiley & Sons, Ltd., 1997.
7. de Groh, K., Banks, B., McCarthy, C., Rucker, R., Berger, L., and Roberts, L., "Analysis of the MISSE PEACE Polymers International Space Station Environmental Exposure Experiment," Paper presented at the 10th International Symposium on Materials in a Space Environment, Collioure, France, June 19–23, 2006.

REPORT DOCUMENTATION PAGE

Form Approved
OMB No. 0704-0188

1. AGENCY USE ONLY (*Leave blank*)	2. REPORT DATE	3. REPORT TYPE AND DATES COVERED
	August 2006	Technical Memorandum

4. TITLE AND SUBTITLE

Comparison of Atomic Oxygen Erosion Yields of Materials at Various Energy and Impact Angles

5. FUNDING NUMBERS

WBS 843515.01.15.03

6. AUTHOR(S)

Bruce A. Banks, Deborah L. Waters, Stephen D. Thorson, Kim K. deGroh, Aaron Snyder, and Sharon Miller

7. PERFORMING ORGANIZATION NAME(S) AND ADDRESS(ES)

National Aeronautics and Space Administration
John H. Glenn Research Center at Lewis Field
Cleveland, Ohio 44135–3191

8. PERFORMING ORGANIZATION REPORT NUMBER

E–15639

9. SPONSORING/MONITORING AGENCY NAME(S) AND ADDRESS(ES)

National Aeronautics and Space Administration
Washington, DC 20546–0001

10. SPONSORING/MONITORING AGENCY REPORT NUMBER

NASA TM—2006-214363

11. SUPPLEMENTARY NOTES

Prepared for the 10th ISMSE and cosponsored by ONERA, CNES, ES, and the 8th International ICPMSE organized by ITL Inc., and CSA, Collioure, France, June 19–23, 2006. Bruce A. Banks, e-mail: Bruce.A.Banks@nasa.gov, Kim K. deGroh, Aaron Snyder, and Sharon Miller, NASA Glenn Research Center; Deborah L. Waters, e-mail: Deborah.L.Waters@nasa.gov, QSS Group, Inc., 21000 Brookpark Rd., Cleveland, Ohio 44135; Stephen D. Thorson, e-mail: sdthorson@wisc.edu, University of Wisconsin at Madison, 1633 Monroe Street, Madison, Wisconsin 53711. Responsible person, Bruce A. Banks, organization code RPY, 216–433–2308.

12a. DISTRIBUTION/AVAILABILITY STATEMENT

Unclassified - Unlimited
Subject Category: 31

Available electronically at http://gltrs.grc.nasa.gov
This publication is available from the NASA Center for AeroSpace Information, 301–621–0390.

12b. DISTRIBUTION CODE

13. ABSTRACT ***(Maximum 200 words)***

The atomic oxygen erosion yields of various materials, measured in volume of material oxidized per incident atomic oxygen atom, are compared to the commonly accepted standard of Kapton H (DuPont) polyimide. The ratios of the erosion yield of Kapton H to the erosion yield of various materials are not consistent at different atomic oxygen energies. Although it is most convenient to use isotropic thermal energy RF plasma ashers to assess atomic oxygen durability, the results can be misleading because the relative erosion rates at thermal energies are not necessarily the same as low Earth orbital (LEO) energies of ~4.5 eV. An experimental investigation of the relative atomic oxygen erosion yields of a wide variety of polymers and carbon was conducted using isotropic thermal energy (~0.1 eV) and hyperthermal energy (~70 eV) atomic oxygen using an RF plasma asher and an end Hall ion source. For hyperthermal energies, the atomic oxygen erosion yields relative to normal incident Kapton H were compared for sweeping atomic oxygen arrival with that of normal incidence arrival. The results of isotropic thermal energy, normal incident, and sweeping incident atomic oxygen are also compared with measured or projected LEO values.

14. SUBJECT TERMS

Chemistry and materials; Polymer matrix composites

15. NUMBER OF PAGES

13

16. PRICE CODE

17. SECURITY CLASSIFICATION OF REPORT	18. SECURITY CLASSIFICATION OF THIS PAGE	19. SECURITY CLASSIFICATION OF ABSTRACT	20. LIMITATION OF ABSTRACT
Unclassified	Unclassified	Unclassified	